

EFFICIENT ROBUST ADAPTIVE BEAMFORMING BASED ON SPATIAL SAMPLING WITH VIRTUAL SENSORS

Saeed Mohammadzadeh Rodrigo C. de Lamare

University of York, UK and CETUC/PUC-Rio, Rio de Janeiro, Brazil

ABSTRACT

Robust adaptive beamforming (RAB) based on interference-plus-noise covariance (IPNC) matrix reconstruction can experience serious performance degradation in the presence of look direction and array geometry mismatches, particularly when the input signal-to-noise ratio (SNR) is large. In this work, we present a RAB technique to address covariance matrix reconstruction problems. The proposed method involves IPNC matrix reconstruction using a low-complexity spatial sampling process (LCSSP) and employs a virtual received array vector. In particular, we devise a power spectrum sampling strategy based on a projection matrix computed in a higher dimension. A key feature of the proposed LCSSP technique is to avoid reconstruction of the IPNC matrix by integrating over the angular sector of the interference-plus-noise region. Simulation results are shown and discussed to verify the effectiveness of the proposed LCSSP method against existing approaches.

Index Terms— Covariance matrix reconstruction, Robust adaptive beamforming, Spatial spectrum process, Virtual Sensors.

1. INTRODUCTION

Many adaptive beamforming methods have been applied in wireless communications, sonar, and radar due to their superior interference mitigation capability [1]. However, under non-ideal conditions such as finite data samples and mismatches between the presumed and true steering vector (SV) the performance of adaptive beamformers degrades substantially. Several RAB techniques have been proposed to enhance robustness against the aforementioned mismatches, such as the linearly constrained minimum variance (LCMV) beamformer [2], diagonal loading (DL) [3, 4, 5, 6, 7, 8], the eigenspace-based beamformer [9, 10], the worst case-based technique [11, 12], the probabilistically constrained approach in [13, 14] and the modified robust Capon beamformer in [15]. Hence, the development of low-complexity RAB approaches has been a very active research topic in recent years. Nevertheless, a major cause of performance degradation in adaptive beamforming is the presence of the desired signal component in the training data, especially at high SNR.

To address this issue, many works tried to remove the signal-of-interest (SOI) components by reconstruction of the interference-plus-noise covariance (IPNC) matrix instead of using the sample covariance matrix (SCM). In [16], the IPNC matrix is reconstructed by integrating the nominal SV and the corresponding Capon spectrum over the entire angular sector except the region near the SOI. Several categories of IPNC matrix-based beamformers were then proposed, such as the beamformer in [17], which relies on a correlation coefficient method, the computationally efficient algorithms via low complexity reconstruction in [18, 19, 20], subspace-based algorithms [21, 22, 23, 24], an approach based on spatial power spectrum sampling (SPSS) [25], and the algorithm in [26] which constructs

an IPNC matrix directly from the signal-interference subspace. The robust beamformer in [27] utilizes the orthogonal subspace (OS) to eliminate the component of the SOI from the angle-related bases while in [28] a robust beamformer is proposed based on the principle of maximum entropy power spectrum (MEPS) to reconstruct the IPNC and the desired signal covariance matrices.

In this paper, we develop an effective RAB approach that achieves nearly optimal performance by addressing the inaccurate covariance matrix construction problems with less computations than other approaches in the literature. The essence of the idea is based on IPNC matrix reconstruction using a low-complexity spatial sampling process (LCSSP) and employing virtual sensors. The power spectrum sampling is realized by a proposed projection matrix in a higher dimension. In contrast to previously reported works with IPNC construction, we avoid the reconstruction and estimation of the IPNC matrix by integrating over the angular sector of the interference-plus-noise region. Simulation results are presented to verify the effectiveness of the proposed method while requiring less computational complexity.

This paper is structured as follows. Section 2 introduces the system model and states the problem. Section 3 presents the proposed LCSSP method. Section 4 depicts and discusses the simulation results, whereas Section 5 draws the conclusions.

2. PROBLEM BACKGROUND

Consider a linear antenna array of M sensors with interelement spacing d . The data received at the t^{th} snapshot depicted as $\mathbf{x}(t) = \mathbf{x}_s(t) + \mathbf{x}_i(t) + \mathbf{x}_n(t)$ which is modeled by

$$\mathbf{x}(t) = s(t)\mathbf{a}(\theta_s) + \sum_{p=1}^P i_p(t)\mathbf{a}(\theta_p) + \mathbf{x}_n(t), \quad (1)$$

where P is the number of interfering signals. $s(t)$, $i_p(t)$ and $\mathbf{x}_n(t)$ denote the desired signal, interference signal waveform and noise components, respectively. Assume that the desired signal, interference, and noise are statistically independent from each other. θ_s , θ_p denotes the direction of the desired signal and the p th interference, respectively. The vector $\mathbf{a}(\cdot)$ is the corresponding SV, which has the form $\mathbf{a}(\theta) = \frac{1}{\sqrt{M}} [1, e^{j2\pi\bar{d}\sin\theta}, \dots, e^{j2\pi(M-1)\bar{d}\sin\theta}]^T$, where $\bar{d} = d/\lambda=1/2$, λ is the wavelength, and $(\cdot)^T$ denotes the transpose. Assuming that the SV $\mathbf{a}(\theta_s)$ is known, then for a given beamformer weight vector \mathbf{w} , the beamformer performance is measured by the output signal-to-interference-plus-noise ratio (SINR) as follows

$$\text{SINR} = \sigma_s^2 |\mathbf{w}^H \mathbf{a}(\theta_s)|^2 / \mathbf{w}^H \mathbf{R}_{i+n} \mathbf{w}, \quad (2)$$

where σ_s^2 is the desired signal power, $\mathbf{R}_{i+n} = \mathbf{R}_i + \mathbf{R}_n$ is the IPNC matrix and $(\cdot)^H$ stands for Hermitian transpose. Assuming that the

interfering signals are independent, the covariance matrix of the received signal vector is given by

$$\mathbf{R} = \sigma_s^2 \mathbf{a}(\theta_s) \mathbf{a}^H(\theta_s) + \sum_{p=1}^P \sigma_p^2 \mathbf{a}(\theta_p) \mathbf{a}^H(\theta_p) + \sigma_n^2 \mathbf{I} \quad (3)$$

where σ_n^2 , σ_p^2 and \mathbf{I} represent the power of the white Gaussian noise, of each interference component and the identity matrix, respectively. Assuming that the SV $\mathbf{a}(\theta_s)$ is known precisely, the problem of maximizing the SINR in (2) can be cast as the following optimization problem:

$$\min_{\mathbf{w}} \mathbf{w}^H \mathbf{R}_{i+n} \mathbf{w} \quad \text{s.t.} \quad \mathbf{w}^H \mathbf{a}(\theta_s) = 1. \quad (4)$$

The solution to (4) yields the optimal beamformer given by

$$\mathbf{w}_{\text{opt}} = \mathbf{R}_{i+n}^{-1} \mathbf{a}(\theta_s) / \mathbf{a}^H(\theta_s) \mathbf{R}_{i+n}^{-1} \mathbf{a}(\theta_s). \quad (5)$$

However, in practice the exact IPNC matrix, \mathbf{R}_{i+n} and array covariance matrix, \mathbf{R} are unavailable even in signal-free applications, thus they are replaced by the SCM, $\hat{\mathbf{R}} = (1/K) \sum_{t=1}^K \mathbf{x}(t) \mathbf{x}^H(t)$, where K is the number of snapshots.

3. PROPOSED LCSSP ALGORITHM

When the incident signal is narrowband, the signal varies slowly with time (assuming that the carrier has been removed). In the noise-free case, a single snapshot is adequate as it contains all available information. A snapshot of a narrowband signal $\beta(t)$ arriving from direction ϕ [29] may be expressed as

$$\mathbf{x}(t) = \beta(t) \mathbf{a}(\phi). \quad (6)$$

The vector representation of the array output model as in (1) plays a very crucial role in the development of high-resolution methods for direction of arrival (DoA) estimation. To steer an array to the desired direction, ϕ_0 , we form an inner product of the SV and the array snapshot [30]

$$\mathbf{a}^H(\phi_0) \mathbf{x}(t) = \beta(t) \mathbf{a}^H(\phi_0) \mathbf{a}(\phi). \quad (7)$$

Therefore, the response of the steered array is expressed as an inner product of the SV and the direction vector as

$$g(\phi; \phi_0) = \mathbf{a}^H(\phi_0) \mathbf{a}(\phi) = \frac{1}{M} \sum_{m=0}^{M-1} e^{jm\pi[\sin(\phi) - \sin(\phi_0)]}, \quad (8)$$

where $\phi_0, \phi \in [-\pi/2, \pi/2]$ are the desired direction to which the array is steered and the DoA of a wavefront, respectively. The function $g(\phi; \phi_0)$ is called the selection function or indication function of the SV [25]. Letting $z = [\sin(\phi) - \sin(\phi_0)]M/2 \in [(-1 - \sin(\phi_0))M/2, (1 - \sin(\phi_0))M/2]$, equation (8) can be rewritten as

$$g(z) = \frac{1}{M} \sum_{m=0}^{M-1} e^{j(2\pi/M)mz} = \frac{\sin(\pi z)}{M \sin(\pi z/M)} e^{j \frac{M-1}{M} \pi z}. \quad (9)$$

Note that $\lim_{z \rightarrow 0} g(z) = 1$, and if $\phi_0 \in (-\pi/2, \pi/2)$, the denominator of (9) will be zero only for $z = 0$ ($\phi = \phi_0$), so $g(z)$ has $M - 1$ zeros in the interval $[(-1 - \sin(\phi_0))M/2, (1 - \sin(\phi_0))M/2]$. We denote these $M - 1$ zeros of $g(z)$ and $g(\phi; \phi_0)$ as $z_m = [\sin(\phi_m) - \sin(\phi_0)]M/2$ with $\phi_m = \arcsin(2z_m/M + \sin(\phi_0))$, for $m =$

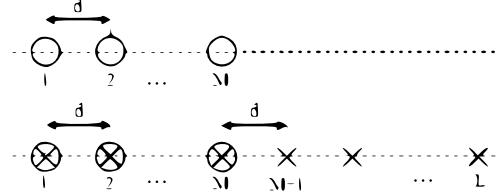


Fig. 1: Virtual and physical array configuration

$1, \dots, M - 1$ respectively. The set $\{\mathbf{a}(\phi_m)\}_{m=0}^{M-1}$ is linearly independent (to see this, note that $\mathbf{A} = [\mathbf{a}(\phi_0) \dots \mathbf{a}(\phi_{M-1})]$ is a Vandermonde matrix with different columns if $\bar{d} \leq 1/2$). This ensures that the SVs of $(\phi_0, \{\phi_m\}_{m=1}^{M-1})$ form an orthonormal basis that spans the M -dimensional complex space.

We intend to construct a projection matrix orthogonal to the signal subspace that retains as much as possible the interference-plus-noise (see (12) below). To this end, it is convenient to extend the array with a number of virtual sensors, as explained next. In Fig. 1, the design of the extended array is shown with $L - M$ virtual sensors.

Let us define an extended received vector as

$$\mathbf{x}_L(t) = \begin{bmatrix} \mathbf{x}(t) \\ \mathbf{x}_e(t) \end{bmatrix}, \quad (10)$$

where $\mathbf{x}(t) = [x_0(t), x_1(t), \dots, x_{M-1}(t)]^T$ is the actual received vector of the array (of dimension M), and the vector received by the virtual part of the extended array (of dimension $L - M$) is depicted as $\mathbf{x}_e(t) = [x_M(t), x_{M+1}(t), \dots, x_L(t)]^T$. Moreover, for the new dimension (L) the corresponding SV of the desired signal $\mathbf{a}_L(\theta_s)$ and the interferences $\mathbf{a}_L(\theta_p)$ are depicted as $\mathbf{a}_L(\theta) = \frac{1}{\sqrt{L}} [1, e^{j2\pi\bar{d}\sin\theta}, \dots, e^{j2\pi(L-1)\bar{d}\sin\theta}]^T$. Thus, the covariance matrix of the extended array's received vector is

$$\begin{aligned} \mathbf{R}_L &= E\{\mathbf{x}_L(t) \mathbf{x}_L^H(t)\} \\ &= E\left\{ \begin{bmatrix} \mathbf{x}(t) \\ \mathbf{x}_e(t) \end{bmatrix} \begin{bmatrix} \mathbf{x}^H(t) & \mathbf{x}_e^H(t) \end{bmatrix} \right\} = \begin{bmatrix} \mathbf{R} & \mathbf{R}_1 \\ \mathbf{R}_1^H & \mathbf{R}_2 \end{bmatrix}, \end{aligned} \quad (11)$$

where \mathbf{R} is the covariance matrix of the original array.

The set of orthogonal SVs with dimension L corresponding to the angles $(\phi_0, \{\phi_\ell\}_{\ell=1}^{L-1})$ spans the L -dimensional complex space. In the following, we show that the IPNC matrix is accurately estimated without resorting to the power spectrum of the interference SVs directly. Instead, we define a projection matrix \mathbf{C}_L onto an approximation to the orthogonal space of the SV of the SOI, taking advantage of the higher dimensions to better approximate the interference-plus-noise space. Assuming $\phi_0 \approx \theta_s$, we use the set of all angles outside the SOI region $\Phi = \{\phi_1, \phi_2, \dots, \phi_\ell, \dots, \phi_{L-1}\}$ to define the orthogonal projection basis. The angles in Φ can then be used to generate the projection matrix as

$$\mathbf{C}_L = \sum_{\phi_\ell \in \Phi} \mathbf{a}(\phi_\ell) \mathbf{a}^H(\phi_\ell), \quad (12)$$

where \mathbf{C}_L is the orthogonal projection matrix onto the span of $\mathbf{a}(\phi_1), \mathbf{a}(\phi_2), \dots, \mathbf{a}(\phi_{L-1})$. Note that if we choose $\phi_0 \approx \theta_s$, $\mathbf{C}_L \mathbf{a}_L(\theta_s) \approx \mathbf{0}$ and if L is sufficiently large, $\mathbf{C}_L \mathbf{a}_L(\theta_p) \approx \mathbf{a}_L(\theta_p)$, $\mathbf{C}_L \mathbf{x}_n \approx \mathbf{x}_n$, as long as the directions θ_p of the interferers are not too close to the direction of the desired signal θ_s . To compute the parameter L in the corresponding interfering signals, the quadratic

error can be minimized in these directions as follows

$$\begin{aligned}\epsilon &= \min_{\mathbf{C}_L} \sum_{p=1}^P \|\mathbf{C}_L \mathbf{a}_L(\theta_p) - \mathbf{a}_L(\theta_p)\|_F^2 \\ &= \|\mathbf{C}_L \mathbf{B}(\theta) - \mathbf{B}(\theta)\|_F^2,\end{aligned}\quad (13)$$

where $\mathbf{B}(\theta) = [\mathbf{a}_L(\theta_1), \dots, \mathbf{a}_L(\theta_P)]$ and $\|\cdot\|_F$ denotes the Frobenius norm. Defining the normalized error as

$$\epsilon_n(\mathbf{C}_L) = \frac{\min \|\mathbf{C}_L \mathbf{B}(\theta) - \mathbf{B}(\theta)\|_F}{\|\mathbf{B}(\theta)\|_F}. \quad (14)$$

the precision can be guaranteed if the error is limited to a small value δ . The best choice for L can be found by computing the error (14), starting from $L = M$ and increasing L until the error is smaller than a prescribed threshold δ .

Let us define

$$\begin{aligned}\mathbf{u} &= \mathbf{C}_L \mathbf{x}_L = \frac{1}{L} \left(\sum_{\ell=1}^{L-1} \mathbf{a}(\phi_\ell) \mathbf{a}^H(\phi_\ell) \right) \left(s(t) \mathbf{a}_L(\theta_s) + \sum_{p=1}^P i_p(t) \right. \\ &\quad \left. \cdot \mathbf{a}_L(\theta_p) + \mathbf{x}_n \right) \approx \sum_{p=1}^P i_p(t) \mathbf{a}_L(\theta_p) + \mathbf{x}_n.\end{aligned}\quad (15)$$

Using these approximations, post-multiplying the above equation by \mathbf{u}^H and taking the expected value of $\mathbf{u} \mathbf{u}^H$, assuming that the interferers $i_p(t)$ are uncorrelated with each other, the signal $s(t)$ and with the noise \mathbf{x}_n , we have

$$\begin{aligned}E\{\mathbf{u} \mathbf{u}^H\} &= E\{\mathbf{C}_L \mathbf{x}_L \mathbf{x}_L^H \mathbf{C}_L^H\} \\ &\approx E\left\{ \left(\sum_{p=1}^P i_p(t) \mathbf{a}_L(\theta_p) + \mathbf{x}_n \right) \left(\sum_{j=1}^P i_j(t) \mathbf{a}_L(\theta_j) + \mathbf{x}_n \right)^H \right\} \\ &= \sum_p \sigma_p^2 \mathbf{a}_L(\theta_p) \mathbf{a}_L^H(\theta_p) + \sigma_n^2 \mathbf{I}.\end{aligned}\quad (16)$$

We can also write

$$\begin{aligned}E\{\mathbf{u} \mathbf{u}^H\} &= \mathbf{C}_L \mathbf{R}_i \mathbf{C}_L^H + \mathbf{C}_L \mathbf{R}_n \mathbf{C}_L^H \\ &= \mathbf{C}_L \mathbf{R}_{i+n}^{(L)} \mathbf{C}_L^H = \begin{bmatrix} \hat{\mathbf{R}}_{i+n} & \mathbf{X}_1 \\ \mathbf{X}_1^H & \mathbf{X}_2 \end{bmatrix}.\end{aligned}\quad (17)$$

The first M entries in \mathbf{x}_L correspond to the physical sensors, which originate the estimate of the $M \times M$ IPNC matrix, $\hat{\mathbf{R}}_{i+n}$, in (17). The matrices \mathbf{X}_1 and \mathbf{X}_2 correspond to the virtual part of the array. The approximation in (15) is effective when $L > M$, resulting in an improved estimate of the IPNC matrix $\hat{\mathbf{R}}_{i+n}$. The robust beamformer is computed by

$$\mathbf{w}_{\text{prop}} = \frac{\hat{\mathbf{R}}_{i+n}^{-1} \mathbf{a}(\bar{\theta}_s)}{\mathbf{a}(\bar{\theta}_s)^H \hat{\mathbf{R}}_{i+n}^{-1} \mathbf{a}(\bar{\theta}_s)}. \quad (18)$$

The computational complexity of the proposed LCSSP algorithm is $\mathcal{O}(M^2 L)$. The solution of the QCQP problem in [16] to obtain the optimal weight vector has complexity of at least $\mathcal{O}(M^{3.5})$, while the beamformer in [27] has a complexity of $\mathcal{O}(SM^3)$ and the reconstructed IPNC matrices in [17] and [25] have a complexity of $\mathcal{O}(M^3)$. Also, the cost of the beamformer in [31] is $\mathcal{O}(\max(M^2 S, M^{3.5}))$ and the beamformer in [28] needs $\mathcal{O}(QM^2)$ complexity where S is the uniform sampling points of the desired signal region.

Algorithm 1 Proposed LCSSP Robust Adaptive Beamforming

```

1: Initialization:  $L=M, \bar{\theta}_s, \phi_0, \delta, \theta_1, \dots, \theta_p$ .
2: Input  $\mathbf{a}_L(\theta), \mathbf{B}$ 
3: For  $L = M : 1 : \dots : \text{Do}$ 
4: Compute Array received data vector  $\{\mathbf{x}_\ell(t)\}_{\ell=1}^L$ ,
5: Compute  $\hat{\mathbf{R}}_L = (1/K) \sum_{t=1}^K \mathbf{x}_L(t) \mathbf{x}_L^H(t)$ ;
6: Define interval as  $\text{Int} = [(-1 - \sin(\phi_0))L/2, (1 - \sin(\phi_0))L/2]$ 
7: Define  $z = \text{Int}(1) : \text{Int}(2)$ 
8:   For  $\ell = 1 : \text{length}(z)$ 
9:      $\phi(\ell) = \arcsin(2z(\ell)/L + \sin(\phi_0))$ 
10:    If  $\phi(\ell) \in \bar{\Theta}$  then
11:       $\mathbf{C}_L = \sum_{\phi(\ell)} \mathbf{a}_L(\phi(\ell)) \mathbf{a}_L^H(\phi(\ell))$ 
12:    end If
13:  End For
14:  Computing the error by (14)
15:  If  $\epsilon_n(\mathbf{C}_L) \leq \delta$  then
16:    Calculate IPNC matrix by (17)
17:    Estimate the IPNC matrix,  $\hat{\mathbf{R}}_{i+n}$  using the first  $M$  row and
18:     $M$  column of (17)
19:  End If
20:  Design proposed beamformer using (18)
21: Output: Proposed beamforming weight vector  $\mathbf{w}_{\text{prop}}$ 

```

4. SIMULATIONS

In this section, a uniform linear array with $M = 10$ omnidirectional sensors is used. Three signals generated from complex white Gaussian noises are considered. It is assumed that there is one desired signal from the presumed direction $\bar{\theta}_s = 0^\circ$ while the uncorrelated interference signals are impinging from -30° and 30° . The proposed LCSSP method is compared with the beamformer in [17] (IPNC-CC), the reconstruction-estimation based beamformer in [16] (IPNC-Est), the beamformer in [27] (IPNC-OS), the beamformer in [25] (IPNC-SPSS), the beamformer in [31] (IPNC-Re) and the beamformer in [28] (IPNC-MEPS). The input interference to noise ratios (INRs) of the two interferers are both set to 30 dB. In the IPNC-CC and IPNC-Est beamformers the number of sampling points for interference-plus-noise region is fixed at 200. In the beamformer IPNC-Re, the upper bound of the norm of the SV mismatch is set to $\sqrt{0.1}$. In the proposed method, we employ $L = 20$, $K = 50$ snapshots, and perform 100 Monte-Carlo runs. The angular sector of the desired signal is set to be $\Theta = [\bar{\theta}_s - 6^\circ, \bar{\theta}_s + 6^\circ]$ where the interference angular sector is $\bar{\Theta} = [-90^\circ, \bar{\theta}_s - 6^\circ] \cup (\bar{\theta}_s + 6^\circ, 90^\circ]$.

In the first example, we compare the beam patterns of the reconstructed IPNC methods. We assume that the input SNR is fixed at 10 dB. Fig. 2 illustrates that all tested beamformers can steer the mainlobe to $\theta_s = 0^\circ$. However, in the proposed LCSSP beamformer the desired signal is preserved and the interferers are effectively suppressed as the depth of the nulls is larger, which indicates that the interference suppression of LCSSP outperforms other methods.

In the second example, we evaluate the proposed method in the presence of the look direction mismatch and model mismatches due to the sensor displacement errors. In this example, the INR is fixed at 10 dB and it is assumed that the desired signal and the interferers are uniformly distributed in $[-6^\circ, 6^\circ]$ while the difference between the actual and assumed SV is modeled as array geometry errors, assuming the sensor position is drawn uniformly from $[-0.05, 0.05]$ wavelength. Note that the DoA of the desired signal and the actual sensor position changes from run to run while remaining constant

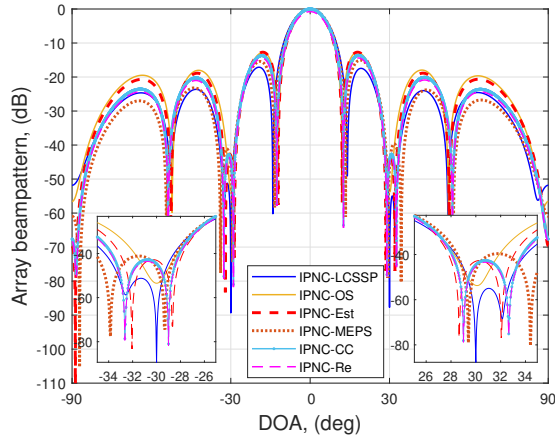


Fig. 2: Comparison of the normalized beampatterns

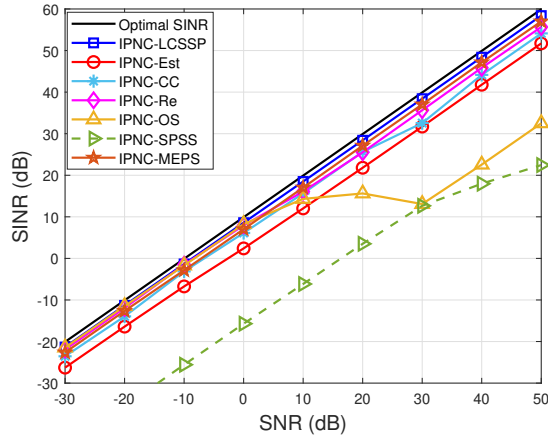


Fig. 3: Output SINR versus Input SNR

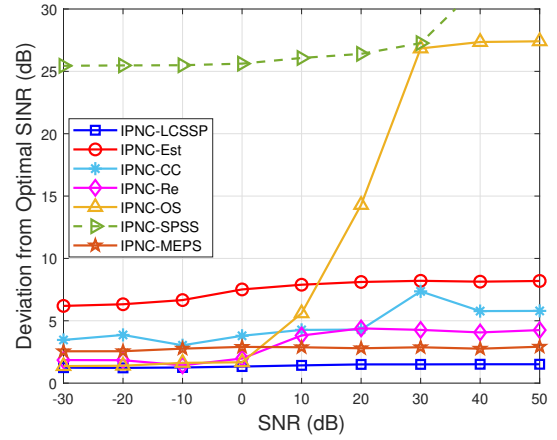


Fig. 4: Deviation from optimal SINR versus SNR

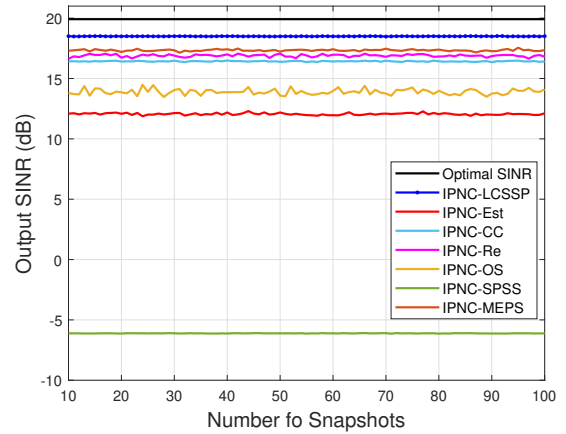


Fig. 5: Output SINR versus Number of Snapshots

over samples. In Fig. 3, we compare the SINR performance versus the SNR where the number of snapshots is fixed at $K = 50$. Since the difference from the optimal SINR at low SNRs is not discernible, the deviations from the optimal SINR are displayed in Fig. 4. From the results, it is observed that, because of random sensor position errors, there is an almost constant performance loss for IPNC-Est and IPNC-CC regardless of the input SNR. At the SNRs higher than 0 dB, the IPNC-Re beamformer has a performance loss because of the look direction mismatch. On the other hand, the proposed LCSSP beamformer almost attains the optimal output SINR under these mismatches for all SNRs. In Fig. 5, the performance of all tested beamformers is examined as the number of snapshots is increased. The excellent performance of LCSSP stems from its highly accurate estimate of the IPNC matrix without any signal power estimation, which enhances the robustness of IPNC-LCSSP against random look direction and array geometry errors over the snapshots. In Fig. 6, we consider the case when the input INR varies, but the SNR is fixed at 10 dB. Clearly, the proposed LCSSP beamformer approaches the output SINR regardless of the interference power. However, both the IPNC-CC and IPNC-Est beamformers degrade as the interference power increases because of the array mismatch.

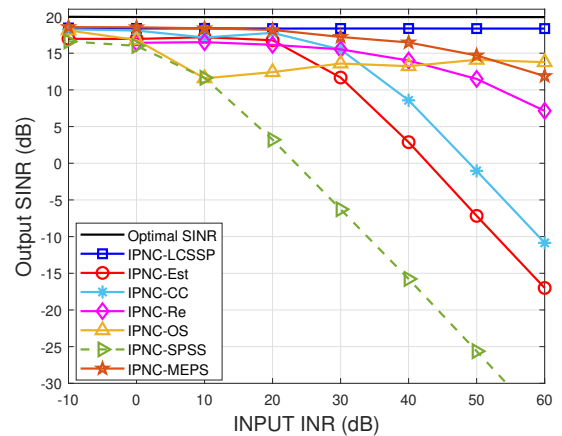


Fig. 6: Output SINR versus input INR

5. CONCLUSION

In this work, an efficient and accurate estimation of the IPNC matrix has been proposed using a low-complexity spatial sampling process

and employing a virtual received array vector. In the proposed LCSSP approach, the power spectrum sampling has been carried out by a projection matrix in a higher dimension. Moreover, the proposed LCSSP approach avoids estimation of the IPNC matrix by integrating over the angular sector of the interference. Simulation results have shown that the proposed LCSSP algorithm outperforms recently reported approaches.

6. REFERENCES

- [1] Harry L Van Trees, *Detection, Estimation, and Modulation Theory*, John Wiley & Sons, New York, 2004.
- [2] Robert A Monzingo and Thomas W Miller, *Introduction to adaptive arrays*, Scitech publishing, 2004.
- [3] O. Kukrer and S. Mohammadzadeh, "Generalised loading algorithm for adaptive beamforming in ulas," *IET Electronics Lett.*, vol. 50, no. 13, pp. 910–912, 2014.
- [4] Z. Yang, R. C. de Lamare, and Xiang Li, " l_1 -regularized stap algorithms with a generalized sidelobe canceler architecture for airborne radar," *IEEE Transactions on Signal Processing*, vol. 60, no. 2, pp. 674–686, 2012.
- [5] L. Wang, R. C. de Lamare, and M. Haardt, "Direction finding algorithms based on joint iterative subspace optimization," *IEEE Transactions on Aerospace and Electronic Systems*, vol. 50, no. 4, pp. 2541–2553, 2014.
- [6] L. Qiu, Y. Cai, R. C. de Lamare, and M. Zhao, "Reduced-rank doa estimation algorithms based on alternating low-rank decomposition," *IEEE Signal Processing Letters*, vol. 23, no. 5, pp. 565–569, 2016.
- [7] Yunlong Cai, R. C. de Lamare, Lie-Liang Yang, and Minjian Zhao, "Robust mmse precoding based on switched relaying and side information for multiuser mimo relay systems," *IEEE Transactions on Vehicular Technology*, vol. 64, no. 12, pp. 5677–5687, 2015.
- [8] V. M. T. Palhares, A. R. Flores, and R. C. de Lamare, "Robust mmse precoding and power allocation for cell-free massive mimo systems," *IEEE Transactions on Vehicular Technology*, vol. 70, no. 5, pp. 5115–5120, 2021.
- [9] Fei Huang, Weixing Sheng, and Xiaofeng Ma, "Modified projection approach for robust adaptive array beamforming," *Signal Process.*, vol. 92, no. 7, pp. 1758–1763, 2012.
- [10] R. Fa and R. C. De Lamare, "Reduced-rank stap algorithms using joint iterative optimization of filters," *IEEE Transactions on Aerospace and Electronic Systems*, vol. 47, no. 3, pp. 1668–1684, 2011.
- [11] S. A. Vorobyov, A. B. Gershman, and Zhi-Quan Luo, "Robust adaptive beamforming using worst-case performance optimization: A solution to the signal mismatch problem," *IEEE Trans. on Signal Process.*, vol. 51, no. 2, pp. 313–324, 2003.
- [12] S. D. Somasundaram, N. H. Parsons, P. Li, and R. C. de Lamare, "Reduced-dimension robust capon beamforming using krylov-subspace techniques," *IEEE Transactions on Aerospace and Electronic Systems*, vol. 51, no. 1, pp. 270–289, 2015.
- [13] Sergiy A Vorobyov, Haihua Chen, and Alex B Gershman, "On the relationship between robust minimum variance beamformers with probabilistic and worst-case distortionless response constraints," *IEEE Trans. on Signal Process.*, vol. 56, no. 11, pp. 5719–5724, 2008.
- [14] Y. Yu, H. Zhao, R. C. de Lamare, Y. Zakharov, and L. Lu, "Robust distributed diffusion recursive least squares algorithms with side information for adaptive networks," *IEEE Transactions on Signal Processing*, vol. 67, no. 6, pp. 1566–1581, 2019.
- [15] Saeed Mohammadzadeh and Osman Kukrer, "Modified robust Capon beamforming with approximate orthogonal projection onto the signal-plus-interference subspace," *Circuits, Systems, and Signal Process.*, pp. 1–18, 2018.
- [16] Y. Gu and A. Leshem, "Robust adaptive beamforming based on interference covariance matrix reconstruction and steering vector estimation," *IEEE Trans. on Signal Process.*, vol. 60, no. 7, pp. 3881–3885, 2012.
- [17] F. Chen, F. Shen, and J. Song, "Robust adaptive beamforming using low-complexity correlation coefficient calculation algorithms," *IET Electronics Lett.*, vol. 51, no. 6, pp. 443–445, 2015.
- [18] Hang Ruan and R. C de Lamare, "Robust adaptive beamforming using a low-complexity shrinkage-based mismatch estimation algorithm," *IEEE Signal Process. Lett.*, vol. 21, no. 1, pp. 60–64, 2014.
- [19] H. Ruan and R. C. de Lamare, "Robust adaptive beamforming based on low-rank and cross-correlation techniques," *IEEE Trans. on Signal Process.*, vol. 64, no. 15, pp. 3919–3932, 2016.
- [20] H. Ruan and R. C. de Lamare, "Distributed robust beamforming based on low-rank and cross-correlation techniques: Design and analysis," *IEEE Transactions on Signal Processing*, vol. 67, no. 24, pp. 6411–6423, 2019.
- [21] R. C. de Lamare and R. Sampaio-Neto, "Reduced-rank adaptive filtering based on joint iterative optimization of adaptive filters," *IEEE Signal Processing Letters*, vol. 14, no. 12, pp. 980–983, 2007.
- [22] R. C. de Lamare and R. Sampaio-Neto, "Adaptive reduced-rank processing based on joint and iterative interpolation, decimation, and filtering," *IEEE Transactions on Signal Processing*, vol. 57, no. 7, pp. 2503–2514, 2009.
- [23] R. Fa, R. C. de Lamare, and L. Wang, "Reduced-rank stap schemes for airborne radar based on switched joint interpolation, decimation and filtering algorithm," *IEEE Transactions on Signal Processing*, vol. 58, no. 8, pp. 4182–4194, 2010.
- [24] Saeed Mohammadzadeh and Osman Kukrer, "Adaptive beamforming based on theoretical interference-plus-noise covariance and direction-of-arrival estimation," *IET Signal Process.*, vol. 12, no. 7, pp. 819–825, 2018.
- [25] Zhenyu Zhang, Wei Liu, Wen Leng, Anguo Wang, and Heping Shi, "Interference-plus-noise covariance matrix reconstruction via spatial power spectrum sampling for robust adaptive beamforming," *IEEE Signal Process. Lett.*, vol. 23, no. 1, pp. 121–125, 2016.
- [26] Peng Chen, Yixin Yang, Yong Wang, and Yuanliang Ma, "Adaptive beamforming with sensor position errors using covariance matrix construction based on subspace bases transition," *IEEE Signal Process. Lett.*, vol. 26, no. 1, pp. 19–23, 2018.
- [27] Yujie Gu and Yimin D Zhang, "Adaptive beamforming based on interference covariance matrix estimation," in *2019 53rd Asilomar Conference on Signals, Systems, and Computers*. IEEE, 2019, pp. 619–623.

- [28] S. Mohammadzadeh, V. H. Nascimento, R. C. de Lamare, and O. Kukrer, "Maximum entropy-based interference-plus-noise covariance matrix reconstruction for robust adaptive beamforming," *IEEE Signal Process. Lett.*, vol. 27, pp. 845–849, 2020.
- [29] Saeed Mohammadzadeh and Osman Kukrer, "Robust adaptive beamforming based on covariance matrix and new steering vector estimation," *Signal, Image and Video Processing*, vol. 13, no. 5, pp. 853–860, 2019.
- [30] Prabhakar S Naidu, *Sensor array signal processing*, CRC press, 2009.
- [31] Zhi Zheng, Yan Zheng, Wen-Qin Wang, and Hongbo Zhang, "Covariance matrix reconstruction with interference steering vector and power estimation for robust adaptive beamforming," *IEEE Trans. on Vehicular Techn.*, vol. 67, no. 9, pp. 8495–8503, 2018.